mathematics

MDPI

Article

The Discovery of Truncated M-Fractional Exact Solitons and a Qualitative Analysis of the Generalized Bretherton Model

Haitham Qawaqneh [1], Khalil Hadi Hakami [2], Ali Altalbe [3,4] and Mustafa Bayram [5,*]

[1] Department of Mathematics, Faculty of Science and Information Technology, Al-Zaytoonah University of Jordan, Amman 11733, Jordan; h.alqawaqneh@zuj.edu.jo
[2] Department of Mathematics, Faculty of Science, Jazan University, P.O. Box 2097, Jazan 45142, Saudi Arabia; khakami@jazanu.edu.sa
[3] Department of Computer Science, Prince Sattam Bin Abdulaziz University, Al-Kharj 11942, Saudi Arabia; a.altalbe@psau.edu.sa
[4] Faculty of Computing and Information Technology, King Abdulaziz University, Jeddah 21589, Saudi Arabia
[5] Department of Computer and Engineering, Biruni University, Istanbul 34010, Turkey
* Correspondence: mustafabayram@biruni.edu.tr

Abstract: This paper is concerned with the novel exact solitons for the truncated M-fractional (1+1)-dimensional nonlinear generalized Bretherton model with arbitrary constants. This model is used to explain the resonant nonlinear interaction between the waves in different phenomena, including fluid dynamics, plasma physics, ocean waves, and many others. A series of exact solitons, including bright, dark, periodic, singular, singular–bright, singular–dark, and other solitons are obtained by applying the extended sinh-Gordon equation expansion (EShGEE) and the modified (G'/G^2)-expansion techniques. A novel definition of fractional derivative provides solutions that are distinct from previous solutions. Mathematica software was used to obtain and verify the solutions. The solutions are shown through 2D, 3D, and density plots. A stability process was conducted to verify that the solutions are exact and accurate. Modulation instability was used to determine the steady-state results for the corresponding equation.

Keywords: generalized Bretherton model; fractional derivatives; stability analysis; modulation instability; analytical methods; exact solitons

MSC: 35Q51; 35R11; 35B35

check for updates

Citation: Qawaqneh, H.; Hakami, K.H.; Altalbe, A.; Bayram, M. The Discovery of Truncated M-Fractional Exact Solitons and a Qualitative Analysis of the Generalized Bretherton Model. *Mathematics* **2024**, *12*, 2772. https://doi.org/10.3390/math12172772

Academic Editor: Raimondas Ciegis

Received: 30 July 2024
Revised: 4 September 2024
Accepted: 5 September 2024
Published: 7 September 2024

1. Introduction

Naturally occurring phenomena are expressed in the form of nonlinear fractional partial differential equations. Many models have been developed in the form of fractional partial differential equations in different fields of science and engineering, including the fractional Phi-4 model [1], the fractional Wazwaz–Benjamin–Bona–Mahony model [2], the fractional regularized long wave model [3], the fractional complex three coupled Maccari's system [4], the fractional paraxial nonlinear Schrödinger model [5], fractional intravenous drug administration [6], the fractional Westervelt model [7], the fractional Single-Joint Robot Arm model [8], the fractional Estevez–Mansfield–Clarkson model [9], the fractional Van der Waals equation [10], and many more.

In this paper, the authors use two simple and useful schemes: the extended sinh-Gordon equation expansion (EShGEE) method and the modified (G'/G^2)-expansion technique. These schemes have been used for different models. The EShGEE technique has been used for the Biswas–Arshed equation [11], the generalized nonlinear Schrödinger equation [12], the novel liquid crystals model [13], a (2+1)-dimensional nonlinear Schrödinger equation with anti-cubic nonlinearity [14], the stochastic Phi-4 equation [15], Klein–Gordon–Zakharov equations [16], the Nizhnik–Novikov–Veselov system [17], the density-dependent

diffusion–reaction equation [18], and the Van der Waals equation [19]. Similarly, the modified (G'/G^2)-expansion scheme has been used for the Fokas–Lenells equation [20], the (1+1)-dimensional classical Boussinesq equation [21], the coupled Drinfel'd–Sokolov–Wilson equation [22], and the Wazwaz–Kaur Boussinesq equation [23].

The basic purpose of our work is to discover the new distinct exact solitons in the (1+1)-dimensional nonlinear generalized Bretherton model, along with a truncated M-fractional derivative. A qualitative analysis of the governing model is also performed.

The motivation for our work is to investigate the novel wave solitons in the generalized Bretherton model. The truncated M-fractional derivative fulfills the characteristics of both integer and fractional derivatives. This definition of derivative provides better solutions than other definitions. First, both of the utilized techniques convert the nonlinear fractional partial differential equations into nonlinear ordinary differential equations (ODEs) and then solve the obtained ODEs. The extended sinh-Gordon equation expansion technique provides the dark, bright, dark–bright, singular, singular–bright, and other solitons. The modified (G'/G^2)-expansion scheme gives the periodic wave, kink soliton, and other types of soliton solutions.

The paper proceeds as follows: the corresponding model and its mathematical treatment are introduced in Section 2, the EShGEE approach and exact solitons are presented in Section 3, the modified (G'/G^2)-expansion technique and its application are detailed in Section 4, a graphical explanation is provided in Section 5, a physical description is offered in Section 6, the stability analysis is described in Section 7, the modulation instability is presented in Section 8, the results and discussion are given in Section 9, and we conclude our work in Section 10.

Truncated M-Fractional Derivative (TMFD)

Definition: Consider $v(x) : [0, \infty) \to \Re$. Therefore, the truncated M-fractional derivative of v of order ϵ [24] is

$$D_{M,x}^{\epsilon,\varrho} v(x) = \lim_{\epsilon \to 0} \frac{v\left(x\, E_\varrho(\epsilon x^{1-\epsilon})\right) - v(x)}{\epsilon}, \quad \epsilon \in (0,1], \quad \varrho > 0,$$

where $E_\varrho(.)$ represents a truncated Mittag–Leffler function [25]

$$E_\varrho(z) = \sum_{j=0}^{i} \frac{z^j}{\Gamma(\varrho j + 1)}, \quad \varrho > 0 \text{ and } z \in \mathbf{C}.$$

Properties: Consider a,b $\in \Re$, and g, f are $\epsilon-$ differentiable at a point $x > 0$; according to [24],

$$(a)\ D_{M,x}^{\epsilon,\varrho}(ag(x) + bf(x)) = aD_{M,x}^{\epsilon,\varrho} g(x) + bD_{M,x}^{\epsilon,\varrho} f(x),$$

$$(b)\ D_{M,x}^{\epsilon,\varrho}(g(x).f(x)) = g(x)D_{M,x}^{\epsilon,\varrho} f(x) + f(x)D_{M,x}^{\epsilon,\varrho} g(x),$$

$$(c)\ D_{M,x}^{\epsilon,\varrho}\left(\frac{g(x)}{f(x)}\right) = \frac{f(x)D_{M,x}^{\epsilon,\varrho} g(x) - g(x)D_{M,x}^{\epsilon,\varrho} f(x)}{(f(x))^2},$$

$$(d)\ D_{M,x}^{\epsilon,\varrho}(B) = 0, \text{ where } B \text{ is a constant},$$

$$(e)\ D_{M,x}^{\epsilon,\varrho} g(x) = \frac{x^{1-\epsilon}}{\Gamma(\varrho + 1)} \frac{dg(x)}{dx}.$$

The truncated M-fractional derivative (TMD) is a fractional derivative that was introduced in Sousa and de Oliveira [25]. This derivative removed the obstacles found in the existing

derivatives. This definition of a derivative is used for various models, such as the Shynaray-IIA equation [26], the Cahn–Allen equation [27], and many more.

2. Model Presentation and Its Mathematical Treatment

Bretherton proposed the following partial differential equation [28]:

$$v_{tt} + v_{xx} + v_{xxxx} + v - v^2 = 0. \tag{1}$$

This is a model of a dispersive wave system to explain the resonant nonlinear interaction between three linear models.

The modified Bretherton equation is given as

$$v_{tt} + v_{xx} + v_{xxxx} + v - v^3 = 0. \tag{2}$$

Equation (2) was used by Kudryashov [29]. Different kinds of solitary wave solutions were obtained in [30,31]. A modified Bretherton equation is considered to further check whether steady-state multiple resonances exist not only for water waves but also for other dispersive media.

Our model is a (1+1)-dimensional nonlinear generalized Bretherton equation with arbitrary constants given as [32]

$$v_{tt} + av_{xx} + bv_{xxxx} + \mu v + cv^3 = 0. \tag{3}$$

Here, $v = v(x,t)$ indicates the wave function, while parameters a, b, c, and μ are arbitrary constants. Equation (3) is discussed using different schemes including the improved (G'/G)-expansion scheme, [32] and the extended tanh-function scheme [33].

The (1+1)-dimensional nonlinear generalized Bretherton model with arbitrary constant in the concept of TMFD is given as

$$D_{M,t}^{2\epsilon,\varrho} v + aD_{M,x}^{2\epsilon,\varrho} v + bD_{M,x}^{4\epsilon,\varrho} v + \mu v + cv^3 = 0. \tag{4}$$

Consider a wave transformation

$$v(x,t) = V(\upsilon), \qquad \upsilon = \frac{\Gamma(1+\varrho)}{\epsilon}(x^\epsilon - \lambda t^\epsilon), \tag{5}$$

where λ is a soliton velocity. Placing Equation (5) in Equation (4) provides

$$\left(a + \lambda^2\right) V'' + bV^{(4)} + cV^3 + \mu V = 0. \tag{6}$$

The natural number m is calculated by applying the homogeneous balance technique into Equation (6), and balancing the terms $V^{(4)}$ and V^3, we obtain $m = 2$.

3. Explanation and Application of the EShGEE Method

3.1. Description

Here, we will mention some of the stages of the scheme.

Stage 1:

We suppose a nonlinear fractional PDE

$$F(g, D_{M,t}^{\epsilon,\varrho} g^2, g^2 g_x, g_x, \ldots) = 0, \tag{7}$$

where $g = g(x,t)$ is a wave profile.

Consider a wave transformation

$$g(x,t) = G(\upsilon), \quad \upsilon = \frac{(1+\varrho)}{\epsilon}(x^\epsilon + \kappa t^\theta). \tag{8}$$

Inserting Equation (8) into Equation (7) yields

$$H(G, G^2G', G'', \ldots) = 0. \tag{9}$$

Stage 2:

Suppose the roots of Equation (9) are as given below:

$$G(f) = \alpha_0 + \sum_{j=1}^{m} (\beta_j \sinh(f) + \alpha_j \cosh(f))^j. \tag{10}$$

Here, α_0, α_j, and β_j $(j = 1, 2, 3, \ldots, m)$ are to be found. Suppose there is a new profile f of $\mho$ that fulfills

$$\frac{df}{d\mho} = \sinh(f). \tag{11}$$

The natural number m is calculated by applying the homogeneous balance scheme. Equation (11) is achieved from the following equation:

$$q_{xt} = \kappa \sinh(v). \tag{12}$$

From [34], we obtain the results for Equation (12):

$$\sinh f(\mho) = \pm \operatorname{csch}(\mho) \quad or \quad \cosh f(\mho) = \pm \coth(\mho), \tag{13}$$

and

$$\sinh f(\mho) = \pm \iota \, sech(\mho) \quad or \quad \cosh f(\mho) = \pm \tanh(\mho). \tag{14}$$

$\iota^2 = -1$.

Stage 3:

Inserting Equation (10) and Equation (11) into Equation (9) results in a system including $f'^k(\mho) \sinh^l f(\mho) \cosh^m f(\mho)$ $(k = 0, 1;\ \ l = 0, 1;\ \ m = 0, 1, 2, \ldots)$. We make each co-efficient of $f'^k(\mho) \sinh^l f(\mho) \cosh^m f(\mho)$ equal to 0, to achieve a set consisting of α_j, $\beta_j (j = 1, 2, 3 \ldots m)$, and others.

Stage 4:

Solving the obtained set yields results for unknowns. From the obtained solutions and Equations (13) and (14), we have the solutions for Equation (9), which are given as

$$G(\mho) = \alpha_0 + \sum_{j=1}^{m} (\pm \beta_j \operatorname{csch}(\mho) \pm \alpha_j \coth(\mho))^j, \tag{15}$$

and

$$G(\mho) = \alpha_0 + \sum_{j=1}^{m} (\pm \iota \beta_j sech(\mho) \pm \alpha_j \tanh(\mho))^j. \tag{16}$$

From this method, one may obtain the sech, csch, tanh, and coth results.

3.2. Application to the EShGEE Scheme

Equation (10) changes to the following form for $m = 2$:

$$V(\mho) = \alpha_0 + \alpha_1 \cosh(f(\mho)) + \beta_1 \sinh(f(\mho)) + (\alpha_2 \cosh(f(\mho)) + \beta_2 \sinh(f(\mho)))^2. \tag{17}$$

Placing Equation (17) into Equation (6) along with Equation (11), we obtain a system containing α_0, α_1, α_2, β_1, β_2, λ, and other parameters. By manumission, we obtain the following sets:

Set 1:

$$\{\alpha_0 = \frac{\sqrt{2b}-\sqrt{-30b}}{\sqrt{c}}, \alpha_1 = 0, \beta_1 = 0, \alpha_2 = \pm\frac{\sqrt[4]{-15}\,2^{3/4}\sqrt[4]{b}}{\sqrt[4]{c}}, \beta_2 = 0,$$
$$\lambda = -\sqrt{-a-2\sqrt{-15}\,b+10b}, \mu = 4(7b-\sqrt{-15}\,b)\}. \quad (18)$$

$$v_1(x,t) = \frac{\sqrt{2b}}{\sqrt{c}}\left(1 \pm \sqrt{-15}\coth(2\frac{\Gamma(1+\varrho)}{\epsilon}(x^\epsilon + \sqrt{-a-2\sqrt{-15}\,b+10b}\,t^\epsilon))\right). \quad (19)$$

$$v_2(x,t) = \frac{\sqrt{2b}}{\sqrt{c}}\left(1 \pm \sqrt{-15}\tanh(2\frac{\Gamma(1+\varrho)}{\epsilon}(x^\epsilon + \sqrt{-a-2\sqrt{-15}\,b+10b}\,t^\epsilon))\right). \quad (20)$$

Set 2:

$$\{\alpha_0 = \frac{\sqrt{2b}-\sqrt{-30b}}{\sqrt{c}}, \alpha_1 = 0, \beta_1 = 0, \alpha_2 = \pm\frac{\sqrt[4]{-15}\,2^{3/4}\sqrt[4]{b}}{\sqrt[4]{c}}, \beta_2 = 0,$$
$$\lambda = \sqrt{-a-2\sqrt{-15}\,b+10b}, \mu = 4(7b-\sqrt{-15}\,b)\}. \quad (21)$$

$$v_1(x,t) = \frac{\sqrt{2b}}{\sqrt{c}}\left(1 \pm \sqrt{-15}\coth(2\frac{\Gamma(1+\varrho)}{\epsilon}(x^\epsilon - \sqrt{-a-2\sqrt{-15}\,b+10b}\,t^\epsilon))\right). \quad (22)$$

$$v_2(x,t) = \frac{\sqrt{2b}}{\sqrt{c}}\left(1 \pm \sqrt{-15}\tanh(2\frac{\Gamma(1+\varrho)}{\epsilon}(x^\epsilon - \sqrt{-a-2\sqrt{-15}\,b+10b}\,t^\epsilon))\right). \quad (23)$$

Set 3:

$$\{\alpha_0 = -\frac{\sqrt{-30b}+\sqrt{2b}}{\sqrt{c}}, \alpha_1 = 0, \beta_1 = 0, \alpha_2 = \pm\frac{\sqrt[4]{-15}2^{3/4}\sqrt[4]{b}}{\sqrt[4]{c}}, \beta_2 = 0,$$
$$\lambda = -\sqrt{-a+10b+2\sqrt{-15}b}, \mu = 4(\sqrt{-15}b+7b)\}. \quad (24)$$

$$v_1(x,t) = \frac{\sqrt{2b}}{\sqrt{c}}\left(-1 \pm \sqrt{-15}\coth(2\frac{\Gamma(1+\varrho)}{\epsilon}(x^\epsilon + \sqrt{-a+10b+2\sqrt{-15}b}\,t^\epsilon))\right). \quad (25)$$

$$v_2(x,t) = \frac{\sqrt{2b}}{\sqrt{c}}\left(-1 \pm \sqrt{-15}\tanh(2\frac{\Gamma(1+\varrho)}{\epsilon}(x^\epsilon + \sqrt{-a+10b+2\sqrt{-15}b}\,t^\epsilon))\right). \quad (26)$$

Set 4:

$$\{\alpha_0 = -\frac{\sqrt{-30b}+\sqrt{2b}}{\sqrt{c}}, \alpha_1 = 0, \beta_1 = 0, \alpha_2 = \pm\frac{\sqrt[4]{-15}2^{3/4}\sqrt[4]{b}}{\sqrt[4]{c}}, \beta_2 = 0,$$
$$\lambda = \sqrt{-a+10b+2\sqrt{-15}b}, \mu = 4(\sqrt{-15}b+7b)\}. \quad (27)$$

$$v_1(x,t) = \frac{\sqrt{2b}}{\sqrt{c}}\left(-1 \pm \sqrt{-15}\coth(2\frac{\Gamma(1+\varrho)}{\epsilon}(x^\epsilon - \sqrt{-a+10b+2\sqrt{-15}b}\,t^\epsilon))\right). \quad (28)$$

$$v_2(x,t) = \frac{\sqrt{2b}}{\sqrt{c}}\left(-1 \pm \sqrt{-15}\tanh(2\frac{\Gamma(1+\varrho)}{\epsilon}(x^\epsilon - \sqrt{-a+10b+2\sqrt{-15}b}\,t^\epsilon))\right). \quad (29)$$

Set 5:

$$\{\alpha_0 = -\frac{2\sqrt{-30b}}{\sqrt{c}}, \alpha_1 = 0, \beta_1 = 0, \alpha_2 = \pm\frac{\sqrt[4]{-15}2^{3/4}\sqrt[4]{b}}{\sqrt[4]{c}}, \beta_2 = 0, \lambda = -\sqrt{-a-20b}, \mu = 64b\}. \quad (30)$$

$$v_1(x,t) = \frac{\left(2\sqrt{-30b}\right)}{\sqrt{c}}\text{csch}^2\left(\frac{\Gamma(1+\varrho)}{\epsilon}(x^\epsilon + \sqrt{-a-20b}\, t^\epsilon)\right). \tag{31}$$

$$v_2(x,t) = -\frac{\left(2\sqrt{-30b}\right)}{\sqrt{c}}\text{sech}^2\left(\frac{\Gamma(1+\varrho)}{\epsilon}(x^\epsilon + \sqrt{-a-20b}\, t^\epsilon)\right). \tag{32}$$

Set 6:

$$\{\alpha_0 = -\frac{2\sqrt{-30b}}{\sqrt{c}}, \alpha_1 = 0, \beta_1 = 0, \alpha_2 = \pm\frac{\sqrt[4]{-15}2^{3/4}\sqrt[4]{b}}{\sqrt[4]{c}}, \beta_2 = 0, \lambda = \sqrt{-a-20b}, \mu = 64b\}. \tag{33}$$

$$v_1(x,t) = \frac{\left(2\sqrt{-30b}\right)}{\sqrt{c}}\text{csch}^2\left(\frac{\Gamma(1+\varrho)}{\epsilon}(x^\epsilon - \sqrt{-a-20b}\, t^\epsilon)\right). \tag{34}$$

$$v_2(x,t) = -\frac{\left(2\sqrt{-30b}\right)}{\sqrt{c}}\text{sech}^2\left(\frac{\Gamma(1+\varrho)}{\epsilon}(x^\epsilon - \sqrt{-a-20b}\, t^\epsilon)\right). \tag{35}$$

4. Explanation of the Modified (G'/G^2)-Expansion Scheme

In this section, we explain the main steps of this scheme [23].

Step 1:

Suppose we have Equations (7)–(9).

Step 2:

Suppose the result for Equation (9) is

$$Q(\upsilon) = \sum_{j=0}^{m} \alpha_j \left(\frac{G'}{G^2}\right)^j, \tag{36}$$

where $\alpha_j (j = 0, 1, 2, 3, \ldots, m)$ are unknowns, while $\alpha_j \neq 0$. The function G = $G(\upsilon)$ fulfills the given ODE,

$$\left(\frac{G'}{G^2}\right)' = \lambda_0 + \lambda_1 \left(\frac{G'}{G^2}\right)^2, \tag{37}$$

where λ_0 and λ_1 are the constants. One can obtain the following cases for Equation (37), depending on the conditions of λ_0:

Case 1: If $\lambda_0\lambda_1 < 0$, then

$$\left(\frac{G'}{G^2}\right) = -\frac{\sqrt{|\lambda_0\lambda_1|}}{\lambda_1} + \frac{\sqrt{|\lambda_0\lambda_1|}}{2}\left[\frac{C_1 \sinh(\sqrt{\lambda_0\lambda_1}\,\upsilon) + C_2 \cosh(\sqrt{\lambda_0\lambda_1}\,\upsilon)}{C_1 \cosh(\sqrt{\lambda_0\lambda_1}\,\upsilon) + C_2 \sinh(\sqrt{\lambda_0\lambda_1}\,\upsilon)}\right]. \tag{38}$$

Case 2: If $\lambda_0\lambda_1 > 0$, then

$$\left(\frac{G'}{G^2}\right) = \sqrt{\frac{\lambda_0}{\lambda_1}}\left[\frac{C_1 \cos(\sqrt{\lambda_0\lambda_1}\,\upsilon) + C_2 \sin(\sqrt{\lambda_0\lambda_1}\,\upsilon)}{C_1 \sin(\sqrt{\lambda_0\lambda_1}\,\upsilon) - C_2 \sin(\sqrt{\lambda_0\lambda_1}\,\upsilon)}\right]. \tag{39}$$

Case 3: If $\lambda_0 = 0$ and $\lambda_1 \neq 0$, then

$$\left(\frac{G'}{G^2}\right) = -\frac{C_1}{\lambda_1(C_1\upsilon + C_2)}. \tag{40}$$

Here, C_1 and C_2 are constants.

Step 3:

We place Equation (36) into Equation (9), along with Equation (37), and we collect the coefficients of every power of $(\frac{G'}{G^2})^j$ to 0; then, solving the algebraic equations, we obtain $\alpha_j, \lambda_0, \lambda_1, \nu$, and others.

Step 4:

Placing Equation (36), in which α_j, ν, and the other parameters were obtained in step 3, into Equation (9), one can obtain the results of Equation (7).

Application

For $m = 2$, Equation (36) reduces into

$$Q(\upsilon) = \alpha_0 + \alpha_1 \frac{G'(\upsilon)}{G^2(\upsilon)} + \alpha_2 (\frac{G'(\upsilon)}{G^2(\upsilon)})^2, \tag{41}$$

where α_0, α_1, and α_2 are unknowns. By substituting Equations (41) and (37) into Equation (6) and solving with Maple software, the following sets of results are obtained:

Set 1:

$$\{\alpha_0 = \pm \frac{2\lambda_0\lambda_1\sqrt{-30\,cb}}{c}, \alpha_1 = 0, \alpha_2 = \pm \frac{2\sqrt{-30\,cb}{\lambda_1}^2}{c}, \lambda = -\sqrt{20\,b\lambda_0\lambda_1 - a}, \mu = 64\,{\lambda_0}^2{\lambda_1}^2 b\}. \tag{42}$$

If $\lambda_0\lambda_1 < 0$, we have

$$v(x,t) = \pm \frac{2\lambda_1\sqrt{-30\,cb}}{c}(\lambda_0 + \lambda_1(-\frac{\sqrt{|\lambda_0\lambda_1|}}{\lambda_1} + \frac{\sqrt{|\lambda_0\lambda_1|}}{2} \ ((C_1 \sinh(\sqrt{\lambda_0\lambda_1}\ \frac{\Gamma(1+\varrho)}{\epsilon} (x^\epsilon + \sqrt{20\,b\lambda_0\lambda_1 - a}\ t^\epsilon)) + C_2 \cosh(\sqrt{\lambda_0\lambda_1}\ \frac{\Gamma(1+\varrho)}{\epsilon}(x^\epsilon + \sqrt{20\,b\lambda_0\lambda_1 - a}\ t^\epsilon)))/(C_1 \cosh(\sqrt{\lambda_0\lambda_1}\ \frac{\Gamma(1+\varrho)}{\epsilon}(x^\epsilon + \sqrt{20\,b\lambda_0\lambda_1 - a}\ t^\epsilon)) + C_2 \sinh(\sqrt{\lambda_0\lambda_1}\ \frac{\Gamma(1+\varrho)}{\epsilon} (x^\epsilon + \sqrt{20\,b\lambda_0\lambda_1 - a}\ t^\epsilon)))))^2). \tag{43}$$

If $\lambda_0\lambda_1 > 0$, we have

$$v(x,t) = \pm \frac{2\lambda_1\sqrt{-30\,cb}}{c}(\lambda_0 + \lambda_1(\sqrt{\frac{\lambda_0}{\lambda_1}}\ ((C_1 \cos(\sqrt{\lambda_0\lambda_1}\ \frac{\Gamma(1+\varrho)}{\epsilon}(x^\epsilon + \sqrt{20\,b\lambda_0\lambda_1 - a}\ t^\epsilon)) + C_2 \sin(\sqrt{\lambda_0\lambda_1}\ \frac{\Gamma(1+\varrho)}{\epsilon}(x^\epsilon + \sqrt{20\,b\lambda_0\lambda_1 - a}\ t^\epsilon)))/(C_1 \sin(\sqrt{\lambda_0\lambda_1}\ \frac{\Gamma(1+\varrho)}{\epsilon} (x^\epsilon + \sqrt{20\,b\lambda_0\lambda_1 - a}\ t^\epsilon)) - C_2 \sin(\sqrt{\lambda_0\lambda_1}\ \frac{\Gamma(1+\varrho)}{\epsilon}(x^\epsilon + \sqrt{20\,b\lambda_0\lambda_1 - a}\ t^\epsilon)))))^2). \tag{44}$$

Set 2:

$$\{\alpha_0 = \pm \frac{2\lambda_0\lambda_1\sqrt{-30\,cb}}{c}, \alpha_1 = 0, \alpha_2 = \pm \frac{2\sqrt{-30\,cb}{\lambda_1}^2}{c}, \lambda = \sqrt{20\,b\lambda_0\lambda_1 - a}, \mu = 64\,{\lambda_0}^2{\lambda_1}^2 b\}. \tag{45}$$

If $\lambda_0\lambda_1 < 0$, we have

$$v(x,t) = \pm \frac{2\lambda_1\sqrt{-30\,cb}}{c}(\lambda_0 + \lambda_1(-\frac{\sqrt{|\lambda_0\lambda_1|}}{\lambda_1} + \frac{\sqrt{|\lambda_0\lambda_1|}}{2} \ ((C_1 \sinh(\sqrt{\lambda_0\lambda_1}\ \frac{\Gamma(1+\varrho)}{\epsilon} (x^\epsilon - \sqrt{20\,b\lambda_0\lambda_1 - a}\ t^\epsilon)) + C_2 \cosh(\sqrt{\lambda_0\lambda_1}\ \frac{\Gamma(1+\varrho)}{\epsilon}(x^\epsilon - \sqrt{20\,b\lambda_0\lambda_1 - a}\ t^\epsilon)))/(C_1 \cosh(\sqrt{\lambda_0\lambda_1}\ \frac{\Gamma(1+\varrho)}{\epsilon}(x^\epsilon - \sqrt{20\,b\lambda_0\lambda_1 - a}\ t^\epsilon)) + C_2 \sinh(\sqrt{\lambda_0\lambda_1}\ \frac{\Gamma(1+\varrho)}{\epsilon} (x^\epsilon - \sqrt{20\,b\lambda_0\lambda_1 - a}\ t^\epsilon)))))^2). \tag{46}$$

If $\lambda_0\lambda_1 > 0$, we have

$$v(x,t) = \pm\frac{2\lambda_1\sqrt{-30\,cb}}{c}(\lambda_0 + \lambda_1(\sqrt{\frac{\lambda_0}{\lambda_1}}\ ((C_1\cos(\sqrt{\lambda_0\lambda_1}\ \frac{\Gamma(1+\varrho)}{\epsilon}(x^\epsilon - \sqrt{20\,b\lambda_0\lambda_1 - a}\ t^\epsilon)) + C_2\sin(\sqrt{\lambda_0\lambda_1}\ \frac{\Gamma(1+\varrho)}{\epsilon}(x^\epsilon - \sqrt{20\,b\lambda_0\lambda_1 - a}\ t^\epsilon)))/(C_1\sin(\sqrt{\lambda_0\lambda_1}\ \frac{\Gamma(1+\varrho)}{\epsilon}(x^\epsilon - \sqrt{20\,b\lambda_0\lambda_1 - a}\ t^\epsilon)) - C_2\sin(\sqrt{\lambda_0\lambda_1}\ \frac{\Gamma(1+\varrho)}{\epsilon}(x^\epsilon - \sqrt{20\,b\lambda_0\lambda_1 - a}\ t^\epsilon)))))^2). \quad (47)$$

Set 3:

$$\{\alpha_0 = \mp\frac{(-\sqrt{-30\,cb} + \sqrt{2}\sqrt{cb})\lambda_1\lambda_0}{c}, \alpha_1 = 0, \alpha_2 = \pm\frac{2\sqrt{-30\,cb}{\lambda_1}^2}{c},$$
$$\lambda = -\frac{\sqrt{-\sqrt{-30\,cb}(30\sqrt{2}\sqrt{cb}\lambda_0\lambda_1 b + 10\,\lambda_0\lambda_1 b\sqrt{-30\,cb} + a\sqrt{-30\,cb})}}{\sqrt{-30\,cb}},$$
$$\mu = \frac{-4{\lambda_0}^2{\lambda_1}^2 b(\sqrt{2}\sqrt{cb} + 9\sqrt{-30\,cb})}{2\sqrt{2}\sqrt{cb} - \sqrt{-30\,cb}}\}. \quad (48)$$

Case 1: If $\lambda_0\lambda_1 < 0$, then

$$v(x,t) = \mp\frac{(-\sqrt{-30\,cb} + \sqrt{2}\sqrt{cb})\lambda_1\lambda_0}{c} \pm \frac{2\sqrt{-30\,cb}{\lambda_1}^2}{c}(-\frac{\sqrt{|\lambda_0\lambda_1|}}{\lambda_1} + \frac{\sqrt{|\lambda_0\lambda_1|}}{2}$$
$$(\frac{C_1\sinh(\sqrt{\lambda_0\lambda_1}\ \frac{\Gamma(1+\varrho)}{\epsilon}(x^\epsilon - \lambda t^\epsilon)) + C_2\cosh(\sqrt{\lambda_0\lambda_1}\ \frac{\Gamma(1+\varrho)}{\epsilon}(x^\epsilon - \lambda t^\epsilon))}{C_1\cosh(\sqrt{\lambda_0\lambda_1}\ \frac{\Gamma(1+\varrho)}{\epsilon}(x^\epsilon - \lambda t^\epsilon)) + C_2\sinh(\sqrt{\lambda_0\lambda_1}\ \frac{\Gamma(1+\varrho)}{\epsilon}(x^\epsilon - \lambda t^\epsilon))})^2. \quad (49)$$

Case 2: If $\lambda_0\lambda_1 > 0$, then

$$v(x,t) = \mp\frac{(-\sqrt{-30\,cb} + \sqrt{2}\sqrt{cb})\lambda_1\lambda_0}{c} \pm \frac{2\sqrt{-30\,cb}{\lambda_1}^2}{c}(\sqrt{\frac{\lambda_0}{\lambda_1}}$$
$$(\frac{C_1\cos(\sqrt{\lambda_0\lambda_1}\ \frac{\Gamma(1+\varrho)}{\epsilon}(x^\epsilon - \lambda t^\epsilon)) + C_2\sin(\sqrt{\lambda_0\lambda_1}\ \frac{\Gamma(1+\varrho)}{\epsilon}(x^\epsilon - \lambda t^\epsilon))}{C_1\sin(\sqrt{\lambda_0\lambda_1}\ \frac{\Gamma(1+\varrho)}{\epsilon}(x^\epsilon - \lambda t^\epsilon)) - C_2\sin(\sqrt{\lambda_0\lambda_1}\ \frac{\Gamma(1+\varrho)}{\epsilon}(x^\epsilon - \lambda t^\epsilon))})^2, \quad (50)$$

where λ is given in Equation (48).

Set 4:

$$\{\alpha_0 = \mp\frac{(-\sqrt{-30\,cb} + \sqrt{2}\sqrt{cb})\lambda_1\lambda_0}{c}, \alpha_1 = 0, \alpha_2 = \pm\frac{2\sqrt{-30\,cb}{\lambda_1}^2}{c},$$
$$\lambda = \frac{\sqrt{-\sqrt{-30\,cb}(30\sqrt{2}\sqrt{cb}\lambda_0\lambda_1 b + 10\,\lambda_0\lambda_1 b\sqrt{-30\,cb} + a\sqrt{-30\,cb})}}{\sqrt{-30\,cb}},$$
$$\mu = \frac{-4{\lambda_0}^2{\lambda_1}^2 b(\sqrt{2}\sqrt{cb} + 9\sqrt{-30\,cb})}{2\sqrt{2}\sqrt{cb} - \sqrt{-30\,cb}}\}. \quad (51)$$

Case 1: If $\lambda_0\lambda_1 < 0$, then

$$v(x,t) = \mp\frac{(-\sqrt{-30\,cb} + \sqrt{2}\sqrt{cb})\lambda_1\lambda_0}{c} \pm \frac{2\sqrt{-30\,cb}{\lambda_1}^2}{c}(-\frac{\sqrt{|\lambda_0\lambda_1|}}{\lambda_1} + \frac{\sqrt{|\lambda_0\lambda_1|}}{2}$$
$$(\frac{C_1\sinh(\sqrt{\lambda_0\lambda_1}\ \frac{\Gamma(1+\varrho)}{\epsilon}(x^\epsilon - \lambda t^\epsilon)) + C_2\cosh(\sqrt{\lambda_0\lambda_1}\ \frac{\Gamma(1+\varrho)}{\epsilon}(x^\epsilon - \lambda t^\epsilon))}{C_1\cosh(\sqrt{\lambda_0\lambda_1}\ \frac{\Gamma(1+\varrho)}{\epsilon}(x^\epsilon - \lambda t^\epsilon)) + C_2\sinh(\sqrt{\lambda_0\lambda_1}\ \frac{\Gamma(1+\varrho)}{\epsilon}(x^\epsilon - \lambda t^\epsilon))})^2. \quad (52)$$

Case 2: If $\lambda_0\lambda_1 > 0$, then

$$v(x,t) = \mp\frac{(-\sqrt{-30\,cb}+\sqrt{2}\sqrt{cb})\lambda_1\lambda_0}{c} \pm \frac{2\sqrt{-30\,cb}{\lambda_1}^2}{c}(\sqrt{\frac{\lambda_0}{\lambda_1}} \left(\frac{C_1\cos(\sqrt{\lambda_0\lambda_1}\,\frac{\Gamma(1+\varrho)}{\epsilon}(x^\epsilon-\lambda t^\epsilon))+C_2\sin(\sqrt{\lambda_0\lambda_1}\,\frac{\Gamma(1+\varrho)}{\epsilon}(x^\epsilon-\lambda t^\epsilon))}{C_1\sin(\sqrt{\lambda_0\lambda_1}\,\frac{\Gamma(1+\varrho)}{\epsilon}(x^\epsilon-\lambda t^\epsilon))-C_2\sin(\sqrt{\lambda_0\lambda_1}\,\frac{\Gamma(1+\varrho)}{\epsilon}(x^\epsilon-\lambda t^\epsilon))}\right))^2, \quad (53)$$

where λ is given in Equation (51).

Set 5:

$$\{\alpha_0 = \mp\frac{(\sqrt{2}\sqrt{cb}+\sqrt{-30\,cb})\lambda_1\lambda_0}{c}, \alpha_1 = 0, \alpha_2 = \mp\frac{2\sqrt{-30\,cb}{\lambda_1}^2}{c}, \lambda = -\frac{\sqrt{\sqrt{-30\,cb}(30\sqrt{2}\sqrt{cb}\lambda_0\lambda_1 b - 10\,\lambda_0\lambda_1 b\sqrt{-30\,cb} - a\sqrt{-30\,cb})}}{\sqrt{-30\,cb}}, \mu = -4\,\frac{{\lambda_0}^2{\lambda_1}^2 b(\sqrt{2}\sqrt{cb}-9\sqrt{-30\,cb})}{2\sqrt{2}\sqrt{cb}+\sqrt{-30\,cb}}\}. \quad (54)$$

Case 1: If $\lambda_0\lambda_1 < 0$, then

$$v(x,t) = \mp\frac{(\sqrt{2}\sqrt{cb}+\sqrt{-30\,cb})\lambda_1\lambda_0}{c} \mp \frac{2\sqrt{-30\,cb}{\lambda_1}^2}{c}(-\frac{\sqrt{|\lambda_0\lambda_1|}}{\lambda_1}+\frac{\sqrt{|\lambda_0\lambda_1|}}{2} \left(\frac{C_1\sinh(\sqrt{\lambda_0\lambda_1}\,\frac{\Gamma(1+\varrho)}{\epsilon}(x^\epsilon-\lambda t^\epsilon))+C_2\cosh(\sqrt{\lambda_0\lambda_1}\,\frac{\Gamma(1+\varrho)}{\epsilon}(x^\epsilon-\lambda t^\epsilon))}{C_1\cosh(\sqrt{\lambda_0\lambda_1}\,\frac{\Gamma(1+\varrho)}{\epsilon}(x^\epsilon-\lambda t^\epsilon))+C_2\sinh(\sqrt{\lambda_0\lambda_1}\,\frac{\Gamma(1+\varrho)}{\epsilon}(x^\epsilon-\lambda t^\epsilon))}\right))^2. \quad (55)$$

Case 2: If $\lambda_0\lambda_1 > 0$, then

$$v(x,t) = \mp\frac{(\sqrt{2}\sqrt{cb}+\sqrt{-30\,cb})\lambda_1\lambda_0}{c} \mp \frac{2\sqrt{-30\,cb}{\lambda_1}^2}{c}(\sqrt{\frac{\lambda_0}{\lambda_1}} \left(\frac{C_1\cos(\sqrt{\lambda_0\lambda_1}\,\frac{\Gamma(1+\varrho)}{\epsilon}(x^\epsilon-\lambda t^\epsilon))+C_2\sin(\sqrt{\lambda_0\lambda_1}\,\frac{\Gamma(1+\varrho)}{\epsilon}(x^\epsilon-\lambda t^\epsilon))}{C_1\sin(\sqrt{\lambda_0\lambda_1}\,\frac{\Gamma(1+\varrho)}{\epsilon}(x^\epsilon-\lambda t^\epsilon))-C_2\sin(\sqrt{\lambda_0\lambda_1}\,\frac{\Gamma(1+\varrho)}{\epsilon}(x^\epsilon-\lambda t^\epsilon))}\right))^2, \quad (56)$$

where λ is given in Equation (54).

Set 6:

$$\{\alpha_0 = \mp\frac{(\sqrt{2}\sqrt{cb}+\sqrt{-30\,cb})\lambda_1\lambda_0}{c}, \alpha_1 = 0, \alpha_2 = \mp\frac{2\sqrt{-30\,cb}{\lambda_1}^2}{c}, \lambda = \frac{\sqrt{\sqrt{-30\,cb}(30\sqrt{2}\sqrt{cb}\lambda_0\lambda_1 b - 10\,\lambda_0\lambda_1 b\sqrt{-30\,cb} - a\sqrt{-30\,cb})}}{\sqrt{-30\,cb}}, \mu = -4\,\frac{{\lambda_0}^2{\lambda_1}^2 b(\sqrt{2}\sqrt{cb}-9\sqrt{-30\,cb})}{2\sqrt{2}\sqrt{cb}+\sqrt{-30\,cb}}\}. \quad (57)$$

Case 1: If $\lambda_0\lambda_1 < 0$, then

$$v(x,t) = \mp\frac{(\sqrt{2}\sqrt{cb}+\sqrt{-30\,cb})\lambda_1\lambda_0}{c} \mp \frac{2\sqrt{-30\,cb}{\lambda_1}^2}{c}(-\frac{\sqrt{|\lambda_0\lambda_1|}}{\lambda_1}+\frac{\sqrt{|\lambda_0\lambda_1|}}{2} \left(\frac{C_1\sinh(\sqrt{\lambda_0\lambda_1}\,\frac{\Gamma(1+\varrho)}{\epsilon}(x^\epsilon-\lambda t^\epsilon))+C_2\cosh(\sqrt{\lambda_0\lambda_1}\,\frac{\Gamma(1+\varrho)}{\epsilon}(x^\epsilon-\lambda t^\epsilon))}{C_1\cosh(\sqrt{\lambda_0\lambda_1}\,\frac{\Gamma(1+\varrho)}{\epsilon}(x^\epsilon-\lambda t^\epsilon))+C_2\sinh(\sqrt{\lambda_0\lambda_1}\,\frac{\Gamma(1+\varrho)}{\epsilon}(x^\epsilon-\lambda t^\epsilon))}\right))^2. \quad (58)$$

Case 2: If $\lambda_0\lambda_1 > 0$, then

$$v(x,t) = \mp\frac{(\sqrt{2}\sqrt{cb}+\sqrt{-30\,cb})\lambda_1\lambda_0}{c} \mp \frac{2\sqrt{-30\,cb}{\lambda_1}^2}{c}(\sqrt{\frac{\lambda_0}{\lambda_1}}\ ((C_1\cos(\sqrt{\lambda_0\lambda_1}\ \frac{\Gamma(1+\varrho)}{\epsilon}(x^\epsilon-\lambda t^\epsilon)) + C_2\sin(\sqrt{\lambda_0\lambda_1}\ \frac{\Gamma(1+\varrho)}{\epsilon}(x^\epsilon-\lambda t^\epsilon)))/(C_1\sin(\sqrt{\lambda_0\lambda_1}\ \frac{\Gamma(1+\varrho)}{\epsilon}(x^\epsilon-\lambda t^\epsilon)) - C_2\sin(\sqrt{\lambda_0\lambda_1}\ \frac{\Gamma(1+\varrho)}{\epsilon}(x^\epsilon-\lambda t^\epsilon)))))^2, \quad (59)$$

where λ is given in Equation (57).

5. Graphical Explanation

Here, we show the solutions obtained in 2D, 3D, and contour graphs. The 2D plots are also drawn for different values of ϵ.

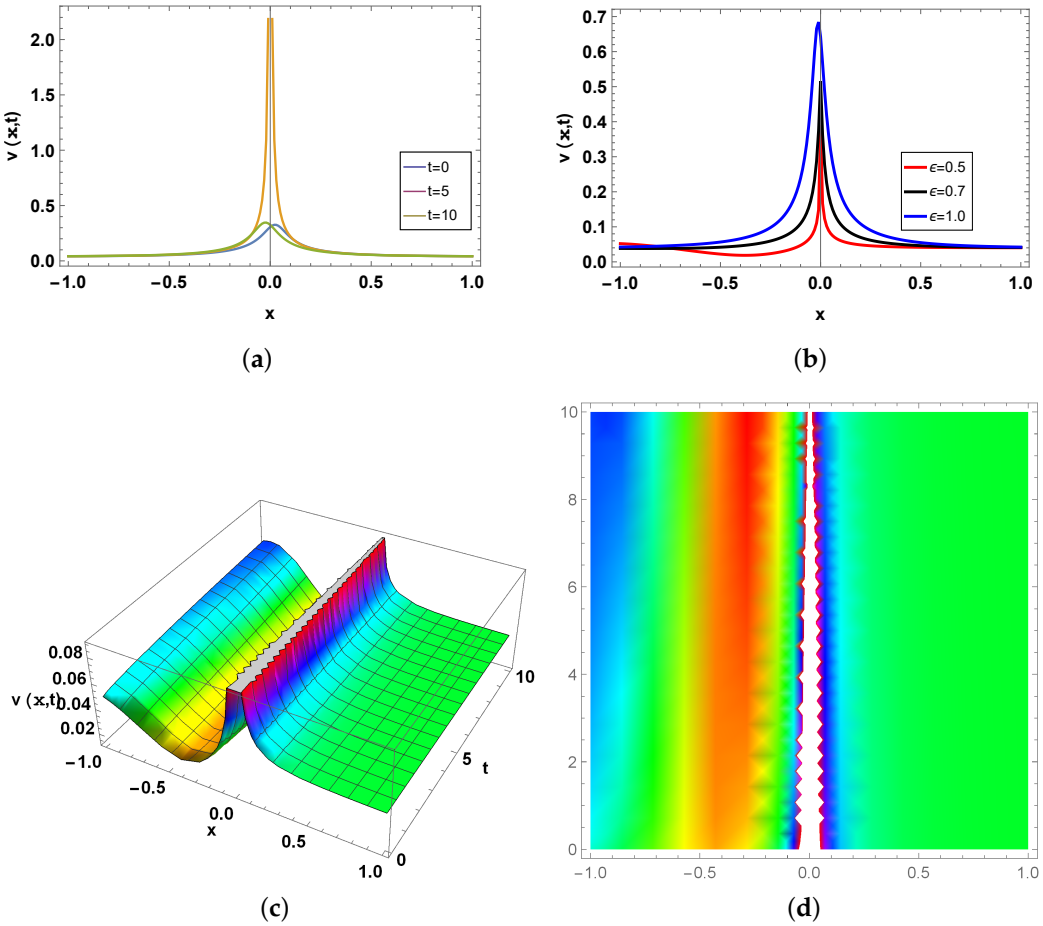

Figure 1. Plot for $v(x,t)$, as shown in Equation (19). (**a**) Two-dimensional plot for distinct values of t. (**b**) Two-dimensional graph for different values of ϵ. (**c**) Three-dimensional graph for $\epsilon = 0.6$. (**d**) Density graph for $\epsilon = 0.6$.

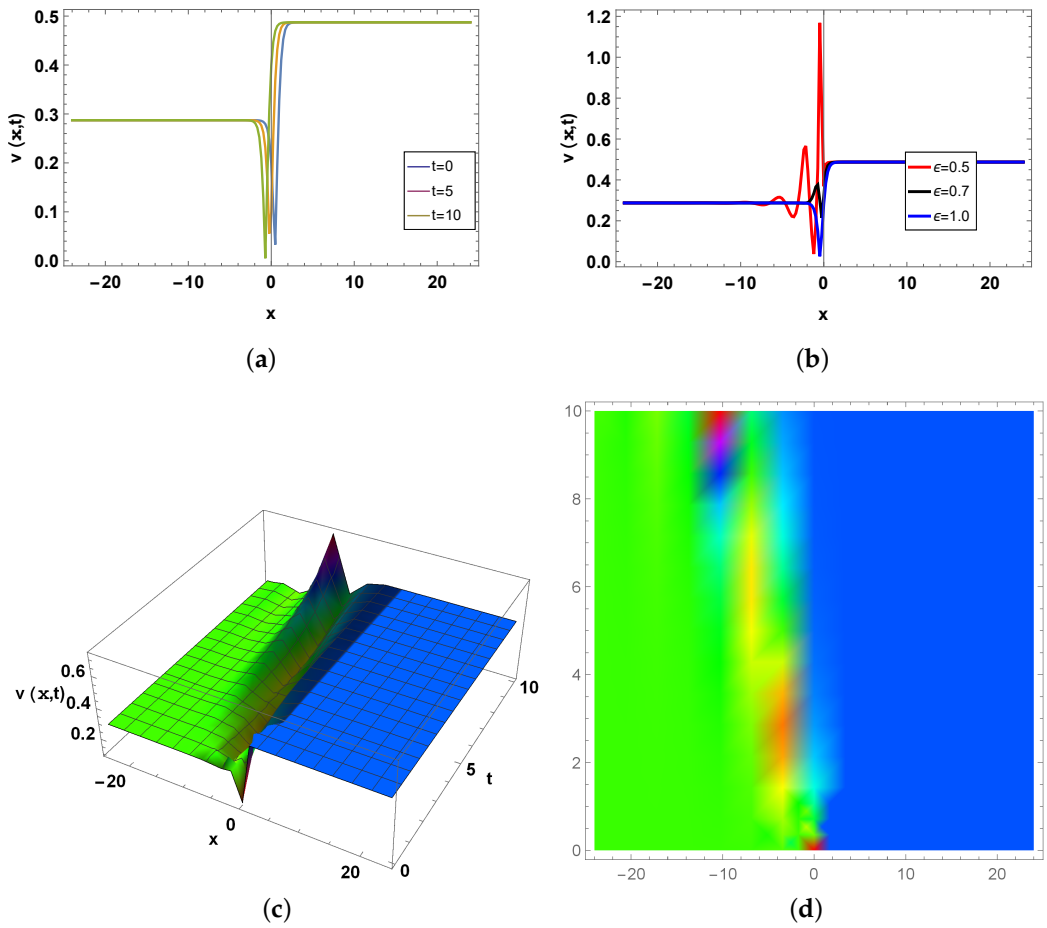

Figure 2. Plot for $v(x,t)$, as shown in Equation (20). (**a**) Two-dimensional plot for distinct values of t. (**b**) Two-dimensional graph for different values of ϵ. (**c**) Three-dimensional graph for $\epsilon = 0.6$. (**d**) Density graph for $\epsilon = 0.6$.

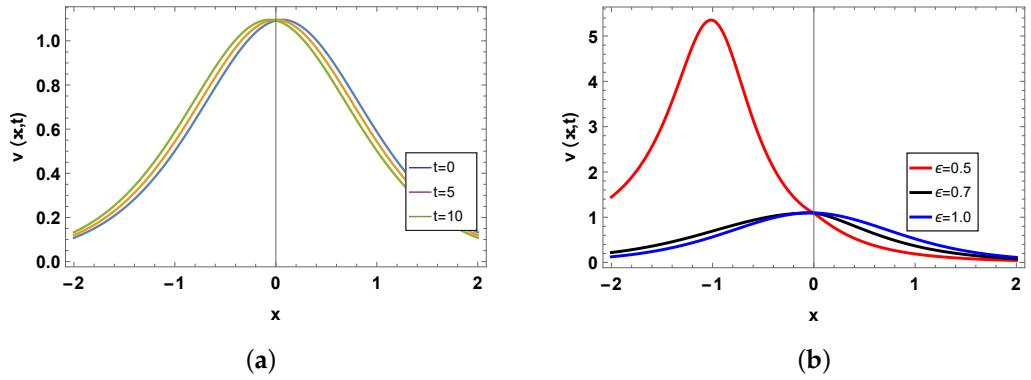

Figure 3. *Cont.*

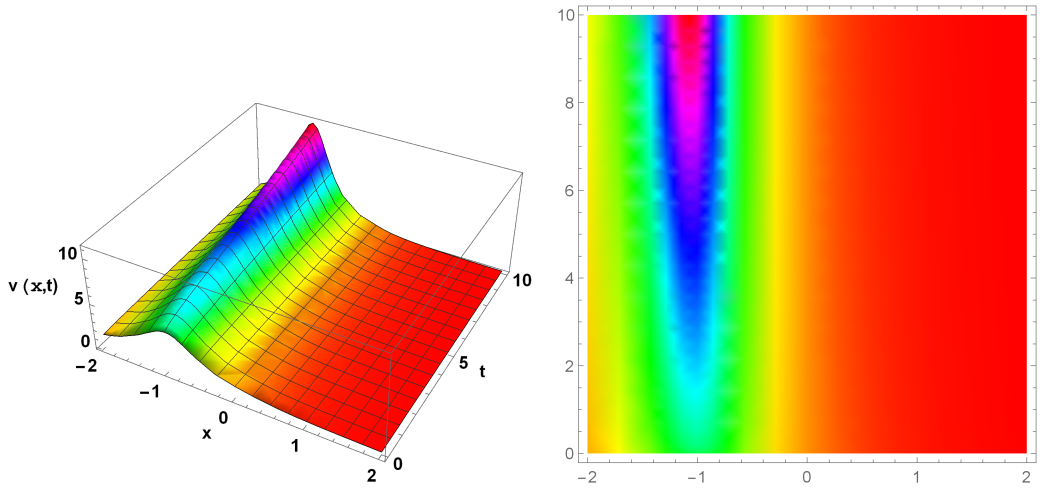

Figure 3. Plot for $v(x,t)$, as shown in Equation (32). (**a**) Two-dimensional graph for different values of t. (**b**) Two-dimensional graph for different values of ϵ. (**c**) Three-dimensional graph for $\epsilon = 0.6$. (**d**) Density graph for $\epsilon = 0.6$.

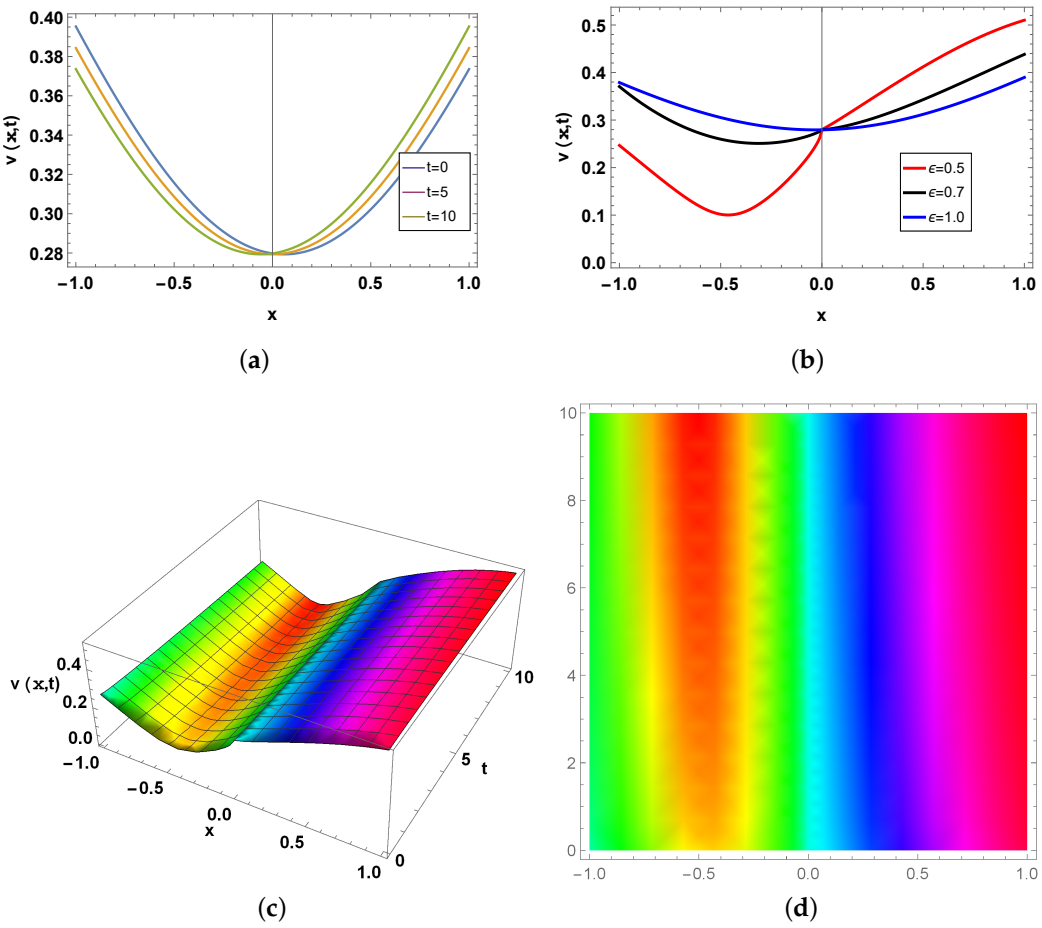

Figure 4. Plot for $v(x,t)$, as shown in Equation (43). (**a**) Two-dimensional plot for distinct values of t. (**b**) Two-dimensional graph for different values of ϵ. (**c**) Three-dimensional graph for $\epsilon = 0.6$. (**d**) Density graph for $\epsilon = 0.6$.

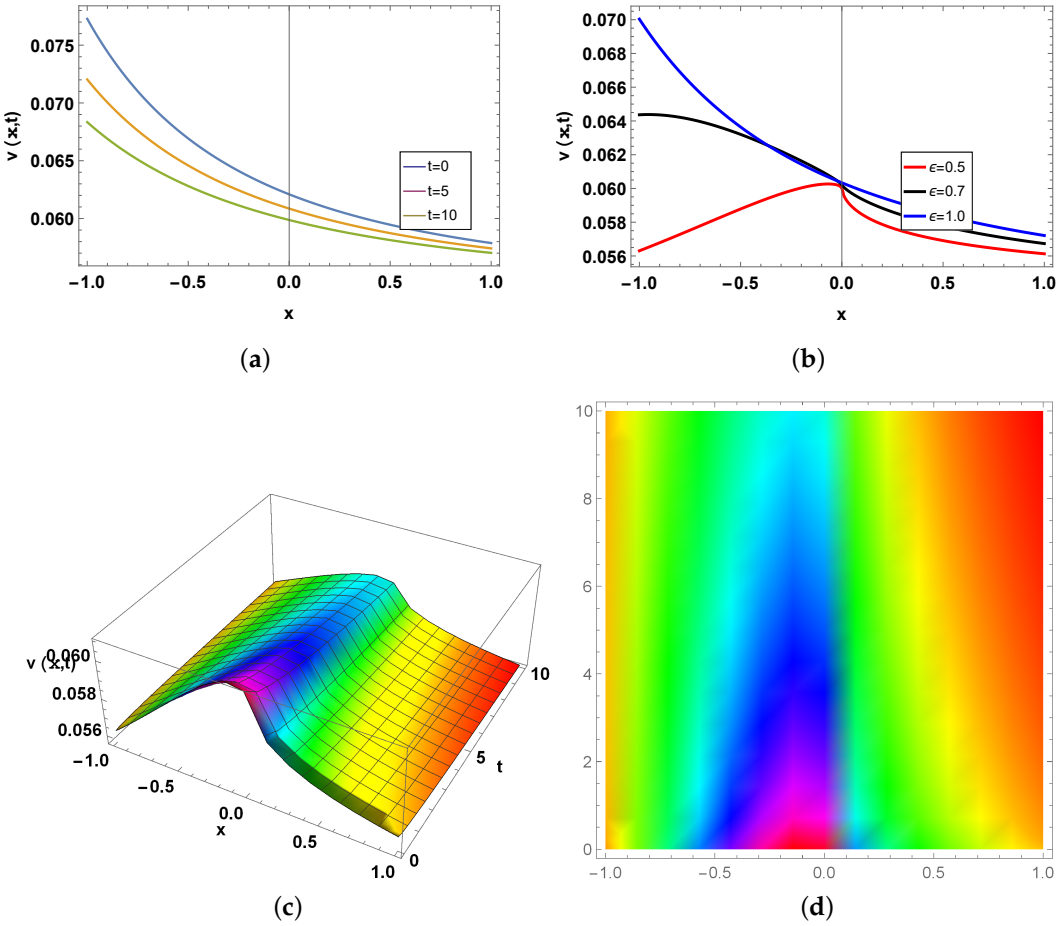

Figure 5. Plot for $v(x,t)$, as shown in Equation (44). (**a**) Two-dimensional plot for distinct values of t. (**b**) Two-dimensional graph for different values of ϵ. (**c**) Three-dimensional graph for $\epsilon = 0.6$. (**d**) Density graph for $\epsilon = 0.6$.

6. Physical Interpretation

Here, we describe the dynamical behavior of the solutions of the truncated M-fractional generalized Bretherton model.

Figure 1 represents a singular soliton at the values of $a = -0.0001, b = -0.0001$, $c = -2$, and $\varrho = 0.5$. Figure 1a represents a 2D graph for $-1 < x < 1$ at $\epsilon = 1$, where the blue line is for $t = 0$, the orange line is for $t = 5$, and the green line is for $t = 10$. Figure 1b represents a two-dimensional graph for $-1 < x < 1$ at $t \in (0, 10)$, where the red line is for $\epsilon = 0.5$, the black line is for $\epsilon = 0.7$, and the blue line is for $\epsilon = 1.0$. Figure 1c represents a three-dimensional graph at $\epsilon = 0.6$ for $t \in (0, 10)$. Figure 1d shows a density plot for $\epsilon = 0.6$ at $t \in (0, 10)$.

Figure 2 represents a dark soliton at the values of $a = 0.005, b = 0.005, c = 1$, and $\varrho = 0.5$. Figure 2a represents a 2D graph for $-24 < x < 24$ at $\epsilon = 1$, where the blue line is for $t = 0$, the orange line is for $t = 5$, and the green line is for $t = 10$. Figure 2b represents a two-dimensional graph for $-24 < x < 24$ at $t \in (0, 10)$, where the red line is for $\epsilon = 0.5$, the black line is for $\epsilon = 0.7$, and the blue line is for $\epsilon = 1.0$. Figure 2c represents a three-dimensional graph at $\epsilon = 0.6$ for $t \in (0, 10)$. Figure 2d shows a density plot for $\epsilon = 0.6$ at $t \in (0, 10)$.

Figure 3 represents a bright soliton at the values of $a = 0.001, b = -0.0001, c = -0.01$, and $\varrho = 0.5$. Figure 3a represents a 2D graph for $-2 < x < 2$ at $\epsilon = 1$, where the blue line is for $t = 0$, the orange line is for $t = 5$, and the green line is for $t = 10$. Figure 3b represents a two-dimensional graph for $-2 < x < 2$ at $t \in (0, 10)$, where the red line is for $\epsilon = 0.5$, the black line is for $\epsilon = 0.7$, and the blue line is for $\epsilon = 1.0$. Figure 3c represents

a three-dimensional graph at $\epsilon = 0.6$ for $t \in (0, 10)$. Figure 3d shows a density plot for $\epsilon = 0.6$ at $t \in (0, 10)$.

Figure 4 represents a kink soliton at the values of $a = 0.0001, b = -0.0001, c = -0.01$, $\lambda_0 = -0.5, \lambda_1 = 1, C_1 = 0.5, C_2 = 0.3$, and $\varrho = 0.5$. Figure 4a represents a 2D graph for $-1 < x < 1$ at $\epsilon = 1$, where the blue line is for $t = 0$, the orange line is for $t = 5$, and the green line is for $t = 10$. Figure 4b represents a two-dimensional graph for $-1 < x < 1$ at $t \in (0, 10)$, where the red line is for $\epsilon = 0.5$, the black line is for $\epsilon = 0.7$, and the blue line is for $\epsilon = 1.0$. Figure 4c represents a three-dimensional graph at $\epsilon = 0.6$ for $t \in (0, 10)$. Figure 4d shows a density plot for $\epsilon = 0.6$ at $t \in (0, 10)$.

Figure 5 represents a periodic wave solution at the values of $a = -0.01, b = 0.0001$, $c = -0.01, \lambda_0 = -0.5, \lambda_1 = -0.1, C_1 = 0.5, C_2 = -0.3$, and $\varrho = 0.5$. Figure 5a represents a 2D graph for $-1 < x < 1$ at $\epsilon = 1$, where the blue line is for $t = 0$, the orange line is for $t = 5$, and the green line is for $t = 10$. Figure 5b represents a two-dimensional graph for $-1 < x < 1$ at $t \in (0, 10)$, where the red line is for $\epsilon = 0.5$, the black line is for $\epsilon = 0.7$, and the blue line is for $\epsilon = 1.0$. Figure 5c represents a three-dimensional graph at $\epsilon = 0.6$ for $t \in (0, 10)$. Figure 5d shows a density plot for $\epsilon = 0.6$ at $t \in (0, 10)$.

7. Stability Analysis

Here, the stability analysis of the model is discussed. It is used to explain how the system behaves in response to external influences over time. Stability analysis was conducted using the properties of a Hamiltonian system tested on some of the obtained solutions to represent the stability of the governing model in terms of application. Stability analysis has been used for many equations, for example, [35,36]. For the stability analysis of Equation (3), one takes the Hamiltonian transformation, given as

$$\mathcal{S} = \frac{1}{2} \int_{-\infty}^{\infty} v^2 \, dx, \tag{60}$$

where $\mathcal{S}$ denotes a momentum factor, while $h(x, t)$ denotes the power of possibility. The necessary condition for the stable solutions is given as

$$\frac{\partial \mathcal{S}}{\partial \lambda} > 0, \tag{61}$$

where λ indicates a wave speed. Inserting Equation (32) into Equation (60) results in

$$\mathcal{S} = \frac{1}{2} \int_{-6}^{6} \left(-\frac{(2\sqrt{-30b})}{\sqrt{c}} \operatorname{sech}^2((x + \sqrt{-a - 20b}\, t))\right)^2 dx, \tag{62}$$

and using the criterion given in Equation (61), we obtain

$$\frac{1920e^{24}(1 - e^{24})bt(4e^{12} \sinh(2t\sqrt{-a - 20b}) + (1 + e^{24}) \sinh(4t\sqrt{-a - 20b}))}{c(2e^{12} \cosh(2t\sqrt{-a - 20b}) + e^{24} + 1)^4} > 0. \tag{63}$$

Hence, Equation (3) denotes a stable nonlinear fractional equation because the condition is satisfied.

8. Modulation Instability (MI)

We take the following transformation for the steady-state result of a generalized Bretherton model [37]:

$$v(x, t) = \left(V(x, t) + \sqrt{\tau}\right) e^{\iota \tau t}, \tag{64}$$

where τ shows the optical power when normalized. Inserting Equation (64) into Equation (3) and linearizing, one obtains

$$aV_{xx} + bV_{xxxx} + \mu\sqrt{\tau} - \tau^{5/2} + 2\iota\tau V_t + V_{tt} + \mu V - \tau^2 V = 0. \tag{65}$$

Consider the solution of Equation (65) in the following form:

$$V(x,t) = A_1 e^{\iota(px-\rho t)} + A_2 e^{-\iota(px-\rho t)}, \tag{66}$$

where ρ and p represent the frequency and normalized wave number of the perturbation, respectively. Putting Equation (66) into Equation (65) and summing up the coefficients of $e^{\iota(px-\rho t)}$ and $e^{\iota(px-\rho t)}$, one obtains the dispersion solution by solving the determinant of the coefficient matrix.

$$a^2p^4 - 2abp^6 - 2a\mu p^2 + 2ap^2\rho^2 + 2ap^2\tau^2 + b^2p^8 + 2b\mu p^4 - 2bp^4\rho^2 - 2bp^4\tau^2 + \mu^2 - 2\mu\rho^2 - 2\mu\tau^2 + \rho^4 - 2\rho^2\tau^2 + \tau^4 = 0. \tag{67}$$

Determining the dispersion solution from Equation (67) for μ results in the following:

$$\mu = \pm 2\rho\tau \pm \sqrt{a^2p^4 - 2abp^6 + 2ap^2\rho^2 + 2ap^2\tau^2 + b^2p^8 - 2bp^4\rho^2 - 2bp^4\tau^2 + \rho^4 + 2\rho^2\tau^2 + \tau^4}. \tag{68}$$

The obtained dispersion form represents the stability of the steady state. If a wave number μ is complex, then the steady state solution will not be stable, because the perturbation grows gradually. If a wave number μ is real, then the steady state remains stable against small perturbations. A steady state result is not stable when

$$a^2p^4 - 2abp^6 + 2ap^2\rho^2 + 2ap^2\tau^2 + b^2p^8 - 2bp^4\rho^2 - 2bp^4\tau^2 + \rho^4 + 2\rho^2\tau^2 + \tau^4 < 0. \tag{69}$$

The MI gain spectrum $G(\rho)$ is achieved as Figure 6

$$\begin{aligned} G(\rho) &= 2Im(\mu) \\ &= \pm\sqrt{a^2p^4 - 2abp^6 + 2ap^2\rho^2 + 2ap^2\tau^2 + b^2p^8 - 2bp^4\rho^2 - 2bp^4\tau^2 + \rho^4 + 2\rho^2\tau^2 + \tau^4}. \end{aligned} \tag{70}$$

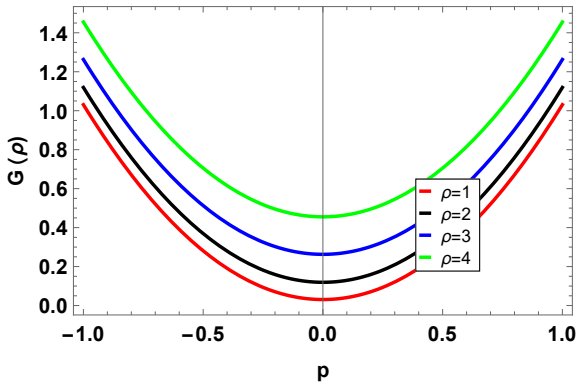

Figure 6. Gain spectrum of MI at different values of ρ.

9. Results and Discussion

Here, we compare the existing results and our results for this model. Different techniques have been used for nonlinear, extended, and modified quantum Zakharov–Kuznetsov equations without fractional derivatives. In [32], the improved (G'/G)-expansion scheme is used to obtain the exact traveling wave solutions. In [33], the an extended tanh-function scheme is utilized to obtain multi soliton-like solutions. However, we consider the model in the truncated M-fractional derivative, which has not been used before in the literature. Furthermore, we utilize the improved (G'/G)-expansion technique to obtain the periodic and kink soliton solutions, while the extended sinh-Gordon equation expansion technique is used to obtain the singular, dark, bright, dark–bright, and many other exact soliton solutions to this model. The obtained solutions have wide applications in different branches of physics and other areas of applied sciences, including fluid dynamics, plasma physics, ocean waves, and many others. Currently, exact solutions, especially soliton-like solutions

have gained importance as a special topic in nonlinear science. Soliton theory has also gained importance because of the exceptional properties of a soliton. A soliton maintains its shape and velocity after interaction and thus its stability.

10. Conclusions

We successfully obtained new kinds of exact solitons for the (1+1)-dimensional nonlinear generalized Bretherton model. A series of exact soliton solutions, including bright, dark, periodic, singular, singular–bright, singular–dark, and other solitons were obtained by applying the extended sinh-Gordon equation expansion (EShGEE) and the modified (G'/G^2)-expansion techniques. A novel definition of the fractional derivative provides solutions distinct from previous solutions. Mathematica software was used to obtain and verify the solutions. The solutions are shown as 2D, 3D, and density graphs. The results are valuable in various areas of applied sciences and engineering. We conclude that the techniques herein are easy to use and provide useful results.

Author Contributions: Methodology, H.Q.; Software, H.Q. and M.B.; Validation, H.Q.; Formal analysis, H.Q. and A.A.; Investigation, A.A. and M.B.; Resources, A.A.; Data curation, K.H.H., A.A. and M.B.; Writing—original draft, K.H.H. and M.B.; Writing—review & editing, K.H.H.; Funding acquisition, K.H.H. All authors have read and agreed to the published version of the manuscript.

Funding: The authors extend their appreciation to Prince Sattam bin Abdulaziz University for funding this research work through the project number (PSAU/2024/01/921063).

Data Availability Statement: No new data were created or analyzed in this study.

Conflicts of Interest: The authors declare no conflicts of interest.

References

1. Ripan, R.; Ali, A.M.; Seadawy, A.R.; Baleanu, D. Search for adequate closed form wave solutions to space—Time fractional nonlinear equations. *Partial. Differ. Equ. Appl. Math.* **2021**, *3*, 100025.
2. Bilal, M.; Ren, J. Dynamics of exact solitary wave solutions to the conformable time-space fractional model with reliable analytical approaches. *Opt. Quantum Electron.* **2022**, *54*, 40. [CrossRef]
3. Behera, S.; Mohanty, S.; Virdi, J.P.S. Analytical solutions and mathematical simulation of traveling wave solutions to fractional order nonlinear equations. *Partial. Differ. Equ. Appl. Math.* **2023**, *8*, 100535. [CrossRef]
4. Alsharidi, A.K.; Bekir, A. Discovery of new exact wave solutions to the M-fractional complex three coupled Maccari's system by Sardar sub-equation scheme. *Symmetry* **2023**, *15*, 1567. [CrossRef]
5. Razzaq, W.; Zafar, A.; Raheel, M. Searching the new exact wave solutions to the beta-fractional Paraxial nonlinear Schrödinger model via three different approaches. *Int. J. Mod. Phys. B* **2024**, *38*, 2450132. [CrossRef]
6. Alijani, Z.; Shiri, B.; Perfilieva, I.; Baleanu, D. Numerical solution of a new mathematical model for intravenous drug administration. *Evol. Intell.* **2024**, *17*, 559–575. [CrossRef]
7. Qawaqneh, H.; Zafar, A.; Raheel, M.; Zaagan, A.A.; Zahran, E.H.M.; Cevikel, A.; Bekir, A. New soliton solutions of M-fractional Westervelt model in ultrasound imaging via two analytical techniques. *Opt. Quantum Electron.* **2024**, *56*, 737. [CrossRef]
8. Batiha, I.M.; Njadat, S.A.; Batyha, R.M.; Zraiqat, A.; Dababneh, A.; Momani, S. Design Fractional-order PID Controllers for Single-Joint Robot Arm Model. *Int. J. Adv. Soft Comput. Its Appl.* **2022**, *14*, 96–114. [CrossRef]
9. Qawaqneh, H.; Alrashedi, Y. Mathematical and Physical Analysis of Fractional Estevez–Mansfield–Clarkson Equation. *Fractal Fract.* **2024**, *8*, 467. [CrossRef]
10. Qawaqneh, H.; Manafian, J.; Alharthi, M.; Alrashedi, Y. Stability Analysis, Modulation Instability, and Beta-Time Fractional Exact Soliton Solutions to the Van der Waals Equation. *Mathematics* **2024**, *12*, 2257. [CrossRef]
11. Zafar, A.; Bekir, A.; Raheel, M.; Razzaq, W. Optical soliton solutions to Biswas–Arshed model with truncated M-fractional derivative. *Optik* **2020**, *222*, 165355. [CrossRef]
12. Bezgabadi, A.S.; Bolorizadeh, M.A. Analytic combined bright-dark, bright and dark solitons solutions of generalized nonlinear Schrödinger equation using extended sinh-Gordon equation expansion method. *Results Phys.* **2021**, *30*, 104852. [CrossRef]
13. Kumar, D.; Joardar, A.K.; Hoque, A.; Paul, G.C. Investigation of dynamics of nematicons in liquid crystals by extended sinh-Gordon equation expansion method. *Opt. Quantum Electron.* **2019**, *51*, 212. [CrossRef]
14. Ilhan, O.A.; Manafian, J. Analytical treatment in optical metamaterials with anti-cubic law of nonlinearity by improved exp (-Ω (*η*))-expansion method and extended sinh-Gordon equation expansion method. *Rev. Mex. Física* **2019**, *65*, 658–677. [CrossRef]
15. Batool, F.; Rezazadeh, H.; Ali, Z.; Demirbilek, U. Exploring soliton solutions of stochastic Phi-4 equation through extended Sinh-Gordon expansion method. *Opt. Quantum Electron.* **2024**, *56*, 785. [CrossRef]

16. Baskonus, H.M.; Sulaiman, T.A.; Bulut, H. On the new wave behavior to the Klein–Gordon–Zakharov equations in plasma physics. *Indian J. Phys.* **2019**, *93*, 393–399. [CrossRef]
17. Cattani, C.; Sulaiman, T.A.; Baskonus, H.M.; Bulut, H. On the soliton solutions to the Nizhnik-Novikov-Veselov and the Drinfel'd-Sokolov systems. *Opt. Quantum Electron.* **2018**, *50*, 138. [CrossRef]
18. Razzaq, W.; Alsharidi, A.K.; Zafar, A.; Alomair, M.A. Optical solitons to the beta-fractional density dependent diffusion-reaction model via three different techniques. *Int. J. Mod. Phys. B* **2023**, *37*, 2350268. [CrossRef]
19. Ali, N.H.; Mohammed, S.A.; Manafian, J. New explicit soliton and other solutions of the Van der Waals model through the EShGEEM and the IEEM. *J. Modern Tech. Eng.* **2023**, *8*, 5–18.
20. Mahak, N.; Akram, G. Exact solitary wave solutions of the (1+1)-dimensional Fokas-Lenells equation. *Optik* **2020**, *208*, 164459. [CrossRef]
21. Aljahdaly, N.H. Some applications of the modified (G'/G^2)-expansion method in mathematical physics. *Results Phys.* **2019**, *13*, 102272. [CrossRef]
22. Behera, S.; Aljahdaly, N.H.; Virdi, J.P.S. On the modified (G'/G^2)-expansion method for finding some analytical solutions of the traveling waves. *J. Ocean. Eng. Sci.* **2022**, *7*, 313–320. [CrossRef]
23. Saboor, A.; Shakeel, M.; Liu, X.; Zafar, A.; Ashraf, M. A comparative study of two fractional nonlinear optical model via modified (G'/G^2)-expansion method. *Opt. Quantum Electron.* **2024**, *56*, 259. [CrossRef]
24. Sulaiman, T.A.; Yel, G.; Bulut, H. M-fractional solitons and periodic wave solutions to the Hirota-Maccari system. *Mod. Phys. Lett. B* **2019**, *33*, 1950052. [CrossRef]
25. Sousa, J.V.D.C.; de Oliveira, E.C. A new truncated M-fractional derivative type unifying some fractional derivative types with classical properties. *Int. J. Anal. Appl.* **2018**, *16*, 83–96.
26. Altalbe, A.; Taishiyeva, A.; Myrzakulov, R.; Bekir, A.; Zaagan, A.A. Effect of truncated M-fractional derivative on the new exact solitons to the Shynaray-IIA equation and stability analysis. *Results Phys.* **2024**, *57*, 107422. [CrossRef]
27. Yao, S.-W.; Manzoor, R.; Zafar, A.; Mustafa, I.; Abbagari, S.; Houwe, A. Exact soliton solutions to the Cahn–Allen equation and Predator–Prey model with truncated M-fractional derivative. *Results Phys.* **2022**, *37*, 105455. [CrossRef]
28. Bretherton, F.P. Resonant interactions between waves. The case of discrete oscillations. *J. Fluidmechanics* **1964**, *20*, 457–479. [CrossRef]
29. Kudryashov, N.A. On types of nonlinear nonintegrable equations with exact solutions. *Phys. Lett. A* **1991**, *155*, 269–275. [CrossRef]
30. Kudryashov, N.A.; Sinelshchikov, D.I.; Demina, M.V. Exact solutions of the generalized Bretherton equation. *Phys. Lett. A* **2011**, *375*, 1074–1079. [CrossRef]
31. Berloff, N.G.; Howard, L.N. Nonlinear wave interactions in nonlinear nonintegrable systems. *Stud. Appl. Math.* **1998**, *100*, 195–213. [CrossRef]
32. Akbar, M.A.; Norhashidah, H.; Mohd, A.; Zayed, E.M.E. Abundant exact traveling wave solutions of generalized Bretherton equation via improved (G'/G)-expansion method. *Commun. Theor. Phys.* **2012**, *57*, 173–178. [CrossRef]
33. Yu, X.; Xu, F.; Zhang, L. Abundant Exact Solition-Like Solutions to the Generalized Bretherton Equation with Arbitrary Constants. *Abstr. Appl. Anal.* **2013**, *7*, 284865. [CrossRef]
34. Yang, X.L.; Tang, J.S. Travelling wave solutions for Konopelchenko-Dubrovsky equation using an extended sinh-Gordon equation expansion method. *Commun. Theor. Phys.* **2008**, *50*, 10471051.
35. Tariq, K.U.; Wazwaz, A.-M.; Javed, R. Construction of different wave structures, stability analysis and modulation instability of the coupled nonlinear Drinfel'd–Sokolov–Wilson model. *Chaos Solitons Fractals* **2023**, *166*, 112903. [CrossRef]
36. Zulfiqar, H.; Aashiq, A.; Tariq, K.U.; Ahmad, H.; Almohsen, B.; Aslam, M.; Rehman, H.U. On the solitonic wave structures and stability analysis of the stochastic nonlinear Schrödinger equation with the impact of multiplicative noise. *Optik* **2023**, *289*, 171250. [CrossRef]
37. ur Rehman, S.; Ahmad, J. Modulation instability analysis and optical solitons in birefringent fibers to RKL equation without four wave mixing. *Alex. Eng. J.* **2021**, *60*, 1339–1354. [CrossRef]